Analyst

Accepted Manuscript

This article can be cited before page numbers have been issued, to do this please use: C. Jiang, Y. He and Y. Liu, *Analyst*, 2020, DOI: 10.1039/D0AN00823K.

View Article Online
DOI: 10.1039/D0AN00823K

REVIEW

Recent advances in sensors for electrochemical analysis of nitrate in food and environmental matrices

Received 00th January 20xx,
Accepted 00th January 20xx

DOI: 10.1039/x0xx00000x

Chunbo Jiang, [a] Yinghe He, [a] and Yang Liu*[a]

Nitrate is one of the most common contaminants in food and the environment, which mainly arises from the intense human activities. Electrochemical sensors have been considered as one of the most promising analytical tools for the rapid detection of nitrate in food and environmental matrices due to their quick response, high sensitivity, ease of operation and miniaturisation, and low sample and power consumption. In this review, we summarise advances in sensors for electrochemical analysis of nitrate over the past decade. We also discuss the application of electrochemical sensing systems for the determination of nitrate in the matrices of fresh water, seawater, food, soil and particulate matter.

1. Introduction

Nitrate, which is one of the naturally occurring chemical forms of nitrogen in ecosystems, is generally formed during nitrification process of the nitrogen cycle carried out by microorganisms. Nitrate is also the most common and important part of synthetic fertilisers to benefit the growth of plants, many of which are food for humans and animals. Dietary nitrates have some positive effects on human body, such as improving blood flow, reducing blood pressure and preventing cardiovascular diseases, through being turned into nitric oxide.[1] However, human activities have significantly altered the global nitrogen cycle. In the areas of intense farming in agricultural systems, fertilisers are used extensively to increase plant production, but unused nitrate can leach out of the soil, enter streams and rivers, and ultimately makes its way into drinking water.[2-4] Besides fertiliser runoff, the sources of nitrates in water include leaky cesspools, sewage treatment plants, manure runoff and combustion fossil fuels. Negative effects may take place in the human body with an excessive intake of nitrate, when they enter the food chain via groundwater, surface water, etc. Infants, for instance, if intaking excess nitrate through drinking water, can suffer “blue baby” disease or methemoglobinemia derived from the endogenous conversion of nitrate to nitrite. Although nitrate levels that affect babies are not dangerous for older children and adults, little is known about the possible long-term effects of exposure to high levels of nitrate in drinking water and food. Table 1 shows the guideline limits for nitrate in drinking water and food in the United States (US),[5] the European Union (EU),[6, 7] Australia[8, 9] and World Health Organization (WHO).[10] Nitrate in water can also lead to blooms of algae that deplete oxygen and leave vast "dead zones", where no fish or typical aquatic life can survive. In addition, exposure of nitrate is linked to the endogenous formation of nitrosamines, which may cause cancers in humans and a wide variety of animal species.[11] From an environmental perspective, nitrate in soils contributes to the release of greenhouse gas, i.e. nitrous oxide, through the denitrification process, which is responsible for the global warming and air pollution.[12] Therefore, it is essential to quantitatively analyse nitrate in both food and environmental matrices.

Table 1 Limits for nitrate in drink water and food in the US, the EU, Australia and WHO

	Drink Water		Food
	(mg/L)	(μM)	(mg/kg)
US	44	710	365
EU	50	806	10-500
Australia	50	806	50-500
WHO	50	806	-

Major constraints to the monitoring of nitrate include the complexity of the analytical procedures, the presence of interfering chemicals and the labour-intensive sampling processes.[3] Thus, a sensing platform that can realise routine measurement without relying on traditional laboratory resources is highly desirable. Over the last decade, the development of low-cost portable devices that can be employed for on-site and continuous analysis of nitrate in various media has attracted considerable interest. Electrochemical sensors have been considered as one of the most promising analytical tools to achieve these goals due to their quick response, high sensitivity, ease of operation and miniaturisation. More importantly, electrochemical techniques have low requirement of sample pretreatment and power consumption, which make them promising candidates for the detection of nitrate in various environmental matrices, particularly for in-field applications.

This review provides an overview of recent advances in sensors for electrochemical analysis of nitrate in food and environmental matrices over the last decade. Although there are several reviews on nitrate detection focusing on the techniques or methods[13-18], to the best of our knowledge, none summarised and discussed the research advances from the perspective of the sample matrix. Since the performances of

[a] College of Science and Engineering, James Cook University, Townsville, Queensland 4811, Australia. E-mail: yang.liu11@jcu.edu.au

electrochemical sensors including sensitivity and selectivity are significantly affected by sample matrix, selection of fit-for-purpose sensors in their applications is of great importance. In this review, after a brief introduction of the electrochemical techniques for nitrate analysis, we will classify the electrochemical nitrate sensors developed in the last 10 years based on sample matrix, with a focus on the progress in their applications.

2. Electrochemical Sensors for Nitrate Detection

A central feature of electrochemical methods is the electrode that provides a surface or interface where some form of a charge-transfer process occurs. This process gives rise to potentials and/or currents that can be measured and related to the concentration of the target analytes. For nitrate detection, commonly used electrochemical sensors can be divided into two groups: those that do not involve a current flow in their measurements, known as potentiometric sensors; and those that do at the electrode under potential control, known as voltammetric or amperometric sensors, depending upon the details of the experimental design.[19]

2.1 Voltammetric/amperometric sensors

Generally, a three-electrode system is employed for voltammetric and amperometric detection of nitrate, including a working electrode (WE) where reduction of nitrate takes place, a reference electrode (RE) that ensures the WE potential is applied accurately and a counter electrode (CE) which is vital for a complete circuit for charge transfer. A voltammetric sensor measures current response as a function of applied potential scanning from one preset value to another, while an amperometric sensor records current at a constant potential applied, which can drive the reaction of nitrate reduction. Additionally, various voltammetric techniques including cyclic voltammetry (CV), square wave voltammetry (SWV) and differential pulse voltammetry (DPV) have been applied to increase the sensitivity and selectivity for nitrate analysis.

The voltammetric/amperometric nitrate sensing is based on electrocatalytic reduction of nitrate, which has been studied for decades. The reduction reaction is usually performed on various metallic electrodes (Pt, Pd, Cu, Au, Ag, Pd-Cu, Pd-In, etc.), which leads to the coexistence of many intermediate products such as nitrite, hydrazine, hydroxylamine, ammonia, nitrogen and other oxygen-containing nitrogen species.[20] The discussion of the mechanism of nitrate reduction is beyond the scope of this review, and we refer interested readers to the relevant references.[20-22] Suffice to mention that, in electrocatalytic analysis of nitrate, the analytical performances are highly dependent on the composition and structure of the electrode materials, while other parameters including analyte concentration, interfering ions and matrix pH also have significant impacts on the current responses of the sensors.[20, 22] Table 2 summarises the voltammetric and amperometric nitrate sensors developed over the last decade from the perspective of sample matrices and electrode materials.

From Table 2, it is clear that the selection of catalyst correlates to the pH of the solution of similar matrices. Under acidic conditions, the presence of protons favours the electrocatalytic reduction of nitrate on copper, which has been widely used as a catalyst for voltammetric and amperometric detection of nitrate due to its high electrocatalytic efficiency and low cost.[23] However, high concentrations of protons also favour the hydrogen evolution reaction, which may result in the increase of the background noise.[24, 25] Therefore, mild acidic conditions (pH between 1 and 3) are usually required when using copper as the catalyst. However, the sensing performances can be significantly degraded in chloride-containing media due to the complex reduction processes of nitrate on copper caused by chloride.[26-30]

Since the majority of nitrate matrices of food and environmental samples are neutral or near neutral, the electrochemical reduction of nitrate in neutral solution has been widely studied in developing valtommetric and amperometric sensors, using nitrate reductases,[31, 32] silver[33-44] and copper[45-47] as the catalysts. Nitrate reductases are molybdoenzymes that can reduce nitrate to nitrite with high sensitivity and specificity/selectivity via immobilisation on the electrodes by physical adsorption or chemical bonding. The challenges of nitrate biosensors based on reductases include the oxygen interferences[48, 49], low electron transfer efficiency[32, 50] as well as the high cost and low storage temperature, which limit their practical applications. Compared to nitrate reductase, copper and silver are cost-effective materials for catalytic detection of nitrate in neutral media. Although copper is cheaper than silver, the silver-based electrodes generally exhibit better sensing performance than the copper-based ones (Table 2) in neutral or near neutral media, which may be attributed to the passivation of copper.[22, 51]

Valtammetric and amperometric nitrate sensors working under alkaline conditions have not been investigated extensively due to the catalyst passivation or poisoning,[20-22] as well as the low market demand. In addition, it is noteworthy that the local pH at the WE surface, where the reduction reactions of nitrate occur, may increase with the consumption of protons, which can result in different catalytic mechanisms taking place at the electrode during the analysis, particularly under high nitrate concentrations.[52]

2.2 Potentiometric sensors

Unlike voltammetric and amperometric sensors that are driven by an externally applied potential, potentiometric sensors measure the potential difference between two electrodes, i.e. ion selective electrode (ISE) and RE. The ISE contains an ion selective membrane (ISM) with a certain ionophore allowing only targeted ions to cross the membrane, which determines the sensitivity and specificity of the analysis, while the RE is an essential element to ensure the accuracy and stability of potential measurements.[53] Several reviews have been published on the progress in this field where all-solid-state ISE, as one of the most active topics, has been specially discussed.[53-55] Instead of using internal filling solution in the conventional ISE, an ion-to-electron transducer is employed in the all-solid-state ISE, which brings many benefits including easy maintenance and miniaturisation of sensing devices. The transducer can be incorporated into the ISM or introduced as a separate transducing layer between the ISM and the inner electron conductive substrate. Most of the ion-to-electron transducers are fabricated based on conducting polymers, carbon nanomaterials or their composite materials. Although conductive polymers have been widely used,

View Article Online
DOI: 10.1039/D0AN00827K

they are usually vulnerable to light, CO_2 and O_2, and are prone to generate water layer, which may result in the potential drift.[54, 56] In recent years, carbon materials (carbon black, carbon nanotube, graphene, etc.) have attracted increasing interests as they are insensitive to O_2 or light, and their hydrophobic property could effectively prevent the formation of the water film between the ISM and the conductive substrate, which can greatly improve the stability and sensitivity for analysis of nitrate in various matrices.[54, 57] In addition, RE with stable, accurate and robust properties is also an indispensable part to miniaturised portable potentiometric sensors. Currently, there are two main types of miniaturised REs used for nitrate sensing. One is the conventional Ag/AgCl RE, and the other is the screen-printed Ag/AgCl quasi- or pseudo-RE, which should be used with caution due to the high susceptibility to [Cl^-] and [Ag^+] ions.[58] In Table 3, the performances of the potentiometric nitrate sensors developed over the last decade are summarised based on the sample matrices.

Although nitrate ionophores play significant roles in the specificity of the ISEs, they have not been extensively studied in the last 10 years. In Table 3, most of the sensors were constructed based on three types of nitrate ionophores, which are quaternary ammonium (or phosphonium) compound, nitrate ionophore V and VI. These ionophores have different selection coefficients, which indicate their binding affinity to nitrate over other anions.[59-61] Generally, tridodecylmethylammonium nitrate (TDMAN) is the most classic and popular nitrate ionophore, which may be attributed to its acceptable selectivity with relatively low cost. However, more efforts are required to explore new nitrate ionophores to improve the specificity of nitrate ISEs[62], particularly for the applications in sample matrix with complex mixtures of anions.

3. Applications of Electrochemical Nitrate Sensors in Various Matrices

3.1 Nitrate in fresh water

Both voltammetric/amperometric and potentiometric sensors have been used for the determination of nitrate in fresh water. For voltammetric or amperometric nitrate sensors, the analytical performances of the sensors are highly dependent on the efficiency of catalysts, which can be significantly influenced by the pH of water matrix. Considering that most of the fresh water has a natural pH in the range of 6 to 8, sample pre-treatment will be required for some of the catalysts to achieve the acceptable performances. Potentiometric nitrate sensors, however, are not very sensitive to the natural pH.[63, 64] This section presents first the catalysts developed for voltammetric/amperometric nitrate sensors in neutral, acidic and alkaline water matrices, then discusses the progresses in the application of potentiometric nitrate sensors, both mainly for the past 10 years.

Neutral matrix. Silver nanoparticle aggregates, which can be successfully electrodeposited on the glassy carbon,[34, 43, 44] graphite,[43] gold[22, 35] and carbon electrodes,[36, 42] exhibited unique properties for detection of nitrate in water under neutral conditions. For example, Hu et al.[35] prepared the 3D dendritic silver nanostructures on gold microelectrode by electrodeposition (Fig. 1A). The nanostructured silver showed high catalytic properties for nitrate detection as evidenced by its attractive analytical performances such as good stability for at least 100 measurements (Fig. 1B), wider linear range from 2 µM to 1000 µM and lower LOD of 2 µM as compared with other nitrate sensors applied in fresh water (Table 2). Furthermore, the effect of pH ranging from 5-9 on the peak current was investigated. It was found that the highest current response was achieved at pH 7 (Fig. 1C), suggesting that the silver nanostructured materials are promising for the voltammetric analysis of nitrate in neutral matrix. Inspired by the excellent electrocatalytic properties of Cu-Pd bimetallic catalyst towards nitrate reduction,[65, 66] Gutés et al. [46] constructed an electrode by depositing Pd particles on the epoxy-Cu electrode, which can detect nitrate in neutral media with a linear range of 32-560 µM. It was proposed that the Pd deposition time must be well-controlled to avoid the full coverage of Cu substrate by Pd since the catalytic performance was attributed to the synergetic effect of Pd particles and Cu substrate. In addition to metal-based catalysts, enzymes have also been used as catalysts in the design of voltammetric and amperometric nitrate sensors in neutral waters. Ahmad et al.[32] fabricated a nitrate biosensor based on direct growth of zinc oxide nanorods on a silver electrode followed by the immobilisation of nitrate reductase via a physical adsorption method. The results demonstrated that the proposed electrode showed a wide linear range from 1 µM to 3400 µM with a LOD of 1 µM and retained 97% of its original response after 1-month storage in buffer solution at 4 °C. The excellent performances can be attributed to the high surface area of the vertically grown ZnO

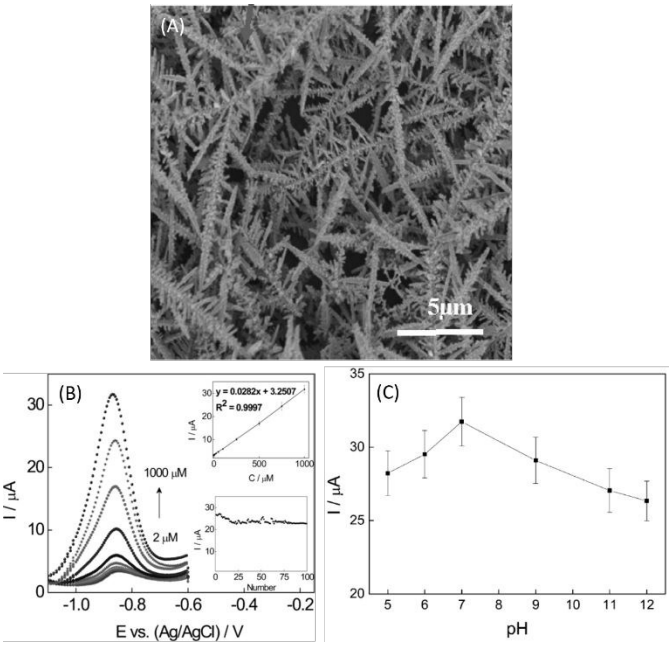

Fig. 1 (A) FE-SEM images of 3D dendritic silver nanostructures on gold microelectrode surfaces; (B) Square wave voltammograms recorded in 2, 5, 10, 25, 50,100, 250, 500, 750 and 1000 mM NaNO3 solutions from down to up. Calibration plot of nitrate based on the peak current taken from the square wave voltammograms are shown in the upper inset. Lower inset: peak current values obtained from successive 100 detections of 750 mM NaNO3 in 0.5 M NaCl; (C) Peak current values of nitrate reduction corresponding to different pH values in 0.5 M NaCl containing 1000 mM NaNO3. Reproduced from ref. 35 with permission from Wiley, copyright 2013.

View Article Online
DOI: 10.1039/D0AN00823K

REVIEW

Table 2 Voltammetric/amperometric sensors for nitrate detection in various matrices

Matrix	Real sample tested	WE and Modified Materials	pH	Linear range (μM)	LOD (μM)	Interference	Durability	Method	Ref.
fresh water	no	Cu nanoclusters, electrodeposited on Pt microelectrode	3	12.5-300	NA	NA	NA	CV	[67]
fresh water	mineral water	Cu microelectrode array	2	10-1070	1.8	NA	50 measurements	SWV	[68]
fresh water	mineral water	Cu nanowire array	1	10-400	1.7-3	nitrite, chloride	NA	LSV	[29]
fresh water	tap and river water	Cu nanowire	2	8-5860	1.35	nitrite	66.7% after 25 days	DPV	[25]
fresh water	pre-treated river water	Cu microspheres decorated on polyaniline on micro-needle	2	20-6000	8	chloride	at least 7 days	DPV	[30]
fresh water	no	Cu nanoparticles electrodeposited on polypyrrole-polystyrene sulfonate-polyethyleneimine-functionalized multiwall carbon nanotubes	7	100-5000	30	NA	NA	CA	[45]
fresh water	spiked tap water	Ag-doped zeolite expanded graphite-epoxy	7	1000-10000	100	NA	NA	CV	[33]
fresh water	no	Ag network-like film on glassy carbon	7	80-6520	3.5	no	92% after 4 weeks	CA	[34]
fresh water	river and lake water	Ag dendritic nanostructure on Au microelectrode array	7	2-1000	2	no	at least 100 measurements	SWV	[35]
fresh water	synthetic aquifer	Ag branchlike on Ag or carbon ultramicroelectrode	7	4-1000	3.2-5.1	no	up to 100 scans	CV	[36]
fresh water	no	Pd nanoparticles on epoxy-Cu	7	32-560	NA	no	NA	CA	[46]
fresh water	no	nitrate reductase/carbon nanotube/polypyrrole, on glassy carbon	7.5	440-1450	170	phenol and glucose	70% after 10 days	CA	[31]
fresh water	tap and pond water	nitrate reductase/ZnO nanorods/Ag electrode	7.4	1-3400	1	no	97% after one month	CA	[32]
fresh water	no	porous Cu-Ni alloy; Rh modified Cu porous layer	7 and 13	20-1000	2.5-12	NA	NA	CA	[47]

View Article Online
DOI: 10.1039/D0AN00823K

fresh water	no	macroporous Ag film on ITO	14	20-5000	NA	no	NA	SWV	[41]
fresh water	no	graphene modified Cu	13	9-940	10	NA	NA	CA	[69]
seawater	synthetic seawater	Ag nanoparticles electrodeposited on Au electrode	5	10-10000	10	NA	NA	CV	[37]
seawater	synthetic seawater	Ag nanoparticles electrodeposited on Au electrode	7	0.39-50	0.39	NA	96% after 26 days	SWV	[38]
seawater	synthetic seawater	Ag nanoparticles electrodeposited on Au electrode	6	$0.9X10^{-3}$ - 1000	$0.9X10^{-3}$	NA	NA	SWV	[39]
soft drink	soft drink, mineral water	Cu sheet by electroplating	2	100-2500	4.2	NA	NA	CA	[70]
food	sausage, cheese (extraction in water)	Cu nanostructure on pencil graphite electrode	2	1-35	0.59	no	NA	CA	[71]
food	Sausage and cheese (extraction in water) mineral water	silver nanoparticles in polypyrrole on glassy carbon	7	2-100	2	no	80% after 60 days	DPV	[40]
food	Sausage, salami and cheese (extraction in water), mineral and tap water	Cu nanoparticles on mixture of multiwall carbon nanotube and reduced graphene oxide on glassy carbon	3	0.1-75	0.02	no	at least 10 SWV scans	SWV	[72]
PM2.5	PM2.5 particles (extraction in water)	Cu deposited on carbon fibre	2	3-2000	1.1	nitrite	at least 10 measurements	SWV	[24]

Table 3 Potentiometric sensors for nitrate detection in various matrices

Matrix	Real sample tested	ISM	Transducer layer	Substrate	Reference electrode	Linear range (M)	LOD (µM)	Potential drift (µV/h)	Lifetime	Ref.
fresh water	mineral and tap water	TDMAN, PVC, o-NPOE	chemically reduced graphene oxide	glassy carbon	Ag/AgCl	10^{-4}-10^{-1}	~50	NA	NA	[73]
fresh water	no	TDMAN, PVC, o-NPOE	carbon black with/without Pt nanoparticles	glassy carbon	Ag/AgCl	10^{-5}-10^{-1}	~0.5	6.3±1.2	6-7 weeks	[57, 74]
fresh water	tap, river, ground and well water	nitrate ionophore V, TDMAC, PVC, o-NPOE,	graphene/TFF-TFF(NO_3)	glassy carbon	Ag/AgCl	10^{-6}-10^{-1}	0.63	NA	NA	[75, 76]
fresh water	no	nitrate ionophore V, TDMAC, PVC, o-NPOE,	TFF-TCNQ	glassy carbon	Ag/AgCl	10^{-5}-10^{-1}	~1.6	17.1	NA	[77]

View Article Online
DOI: 10.1039/D0AN00823K

fresh water	lake, stream and river	TDMAC, PVC, o-NPOE,	graphite (mechamical abrasion from pencils)	graphite via mechamical abrasion from pencils	TBA-TBB, o-NPOE, PVC	10^{-5}-10^{-1}	2.5	NA	NA	78
fresh water	no	nitrate ionophore VI, TDMAC, o-NPOE, PVC	Thiol-functionalized reduced graphene oxide	Au	Ag/AgCl	10^{-5}-10^{-1}	~4	8.79	over 2 weeks	59
fresh water	tap and well water	TDMAN, PVC, dibutyl phthalate	polypyrrole	graphite paste	Ag/AgCl	10^{-5}-10^{-1}	<10	NA	6-12 months	79
seawater	seawater	TDMAN, ETH500, PMMA-PDMA	lipophilic multiwalled carbon nanotubes	glassy carbon	Ag/AgCl, miniatured	NA	3.8±0.1	< 50	NA	80
seawater	seawater	TDMAN, ETH500, PMMA-PDMA	lipophilic multiwalled carbon nanotubes	glassy carbon	Ag/AgCl, miniatured	$5X10^{-5}$–10^{-2}	0.9	500	at least 23h	81
food	mint, lettuce, cabbage, etc. (extraction in water)	TDMAN, dibutyl phthalate, PVC	graphite, epoxy and hardener	copper	Ag/AgCl	10^{-4}-10^{-1}	66	NA	NA	82
food	food (extraction in water), tap and mineral water	THTDPC, PVC, o-NPOE,	THTDPC (incorparated into ISM)	Ag/AgCl electrode	Ag/AgCl	10^{-5}-10^{-1}	2.8	45.8 (1-3 days); 5.9 (3-30 days)	~4 months	83, 84
soil	soil extract and soil slurry	TDMAN, PVC, o-NPOE,	graphene	glassy carbon	Ag/AgCl	NA	~6.3	NA	NA	85
soil	soil slurry	TDMAN, MTPPB, nitrocellulose, o-NPOE, PVC	laser-induced graphene	laser-induced graphene	Ag/AgCl	10^{-5}-10^{-1}	20.6 ±14.8	5.3	NA	86
soil	soil slurry	TDMAN, MTPPB, nitrocellulose, o-NPOE, PVC	poly(3-octyl-thiophene), MoS_2	Au	Ag/AgCl (screen-printed, covered by Nafion)	NA	~22.6	8.33	at least 27 days	87

o-NPOE: o-nitrophenyl octyl ether; PVC: poly (vinyl chloride); TDMAN: tridodecylmethylammonium nitrate; TDMAC: tridodecylmethylammonium chloride; ETH500: tetrakis(4-chlorophenyl)borate tetradodecylammonium salt, PMMA-PDMA: poly(methylmethacrylate-decylmethacrylate); THTDPC: trihexyltetradecylphosphonium chloride; MTPPB: methyltriphenylphosphonium bromide; molybdenum disulphide: MoS_2; TBA-TBB: tetrabutylammonium tetrabutylborate; TFF-TFF(NO_3): tetrathiafulvalene-tetrathiafulvalene-NO_3; TFF-TCNQ: tetrathiafulvalene-tetracyanoquinodimethane;

nanorods, which enabled large amounts of enzymes to be immobilised for the catalytic reduction of nitrate. Furthermore, no obvious interference from common interfering ions in water was observed due to the high specificity of the enzyme-based sensor. Overall, as indicated in Table 2, the sensors constructed with silver or nitrate reductase generally show better performances than those obtained with other catalysts in neutral media.

Acidic matrix. Copper of various structures, such as nano-clusters,[67] dendrites,[88] micro-array,[68] nanowire array,[29] nanowire,[25] micro-sphere,[30] etc. has been employed in voltammetric or amperometric sensors for nitrate detection in acidic media. Compared with the bare copper electrode, the diverse copper structures exhibited higher electrocatalytic activity due to the enhanced specific surface area, resulting in improved analytical performances when applied to the fabrication of nitrate sensors. For example, the copper nanowire electrodes[25] showed better LOD than the microsphere ones[30] (Table 2). It was reported, however, that the presence of nitrite will lead to the formation of nitrite reduction peak at lower negative potential, which could decrease the sensitivity for nitrate analysis with no observed apparent influence on other performances.[25, 29] The presence of chloride was also reported to enhance the peak current density and shift the peak potential towards the more negative side, which must be taken into consideration during the measurements.[29, 30]

Alkaline matrix. Both copper[69] and silver[41] have been employed for voltammetric nitrate sensing under alkaline conditions. Öznülüer et al. developed a graphene-modified copper electrode to measure nitrate in alkaline media.[69] The predominantly single-layer graphene

films were deposited on the copper foils by chemical vapour deposition. Compared with the bare copper electrode, the electrode covered by graphene obtained a wider linear range of 10-940 µM, lower LOD of 10 µM and a much better sensitivity of 173.7 µA/mM/cm^2, which were attributed to the higher catalytic activity towards nitrate reduction as a result of the special surface electronic structure of the Cu/graphene. The stability of the modified electrode was not investigated in this work. Comisso et al. developed bimodal porous Cu, Cu-Ni and Rh-modified Cu electrodes to measure nitrate in basic and neutral water solutions.[47, 89] The porous structure consisting of both macropores and micropores was formed by electrodeposition at high current density, exploiting the transient template action of hydrogen bubbles. The results indicated that the bimodal porous structure could increase the catalytic activity and stability, due to the large surface area and enhanced mass transport. The three porous electrodes showed similar linear ranges and LODs. However, compared with the porous Cu electrode as a benchmark, Rh-modified Cu electrode exhibited 25% to 50% higher sensitivity but lower stability for nitrate detection in basic media; the Cu-Ni electrode was the most stable under basic and neutral conditions, although it was generally less sensitive than the other electrode materials.

Potentiometric sensors, introduced in 1976 for nitrate ion detection in water,[90] are not very sensitive to the pH of fresh water.[63, 64] Most of the recent research has focused on the exploration of new ion-to-electron transducers. Tang et al.[73] developed an all-solid-state nitrate-selective electrode using chemically reduced graphene oxide (CRGNO) as the ion-to-electron transducer to test nitrate in drinking water. The sensor showed a rapid response time (within 10 seconds) for the nitrate concentration between 100 µM and 0.1 M. The authors suggested that graphene could significantly facilitate the ion-to-electron transduction and prevent the formation of water layer between the ISM and the graphene layer because of the hydrophobic property of the CRGNO. However, it was found that the nitrate concentrations measured with this potentiometric sensor were inconsistent with the results obtained with ultraviolet spectrophotometry, particularly for the samples with low concentrations of nitrate, which might be due to some interfering ions in the sample matrix. In addition, Piek et al.[76] used the graphene/tetrathiafulvalene/tetrathiafulvalene-NO_3 nanocomposites as the ion-to-electron transducer, achieving a broader linear range from 1 µM to 0.1 M and a LOD of 0.63 µM after conditioned in 0.1 mM KNO_3 solution. The improved performances were attributed to the high hydrophobicity, large double layer and redox capacitance of the nanocomposites. Another attractive feature of this sensor was the high potential stability with a notable decrease of the potential drift from 16.6 µV/s (applied current 1 nA) to 4.26 µV/s (applied current 5 nA) due to the presence of graphene, although the linear range and LOD were both similar to the results when only tetrathiafulvalene-NO_3 was used as the transducer media.[75] The same group also developed the nitrate-selective electrodes using the organic donor-acceptor, i.e. tetrathiafulvalene-tetracyanoquinodimethane, as the ion-to-electron transducer, which showed poor performance compared with the sensors constructed from the graphene nanocomposites.[77] Recently, Liu et al.[59] employed thiol-functionalised reduced graphene oxide (TRGO) as the ion-to-electron transducing layer to combine with the gold substrate based on the Au-S covalent linkage. The results indicated that the Au-S covalent linkage made the sensor more reliable and reproducible.

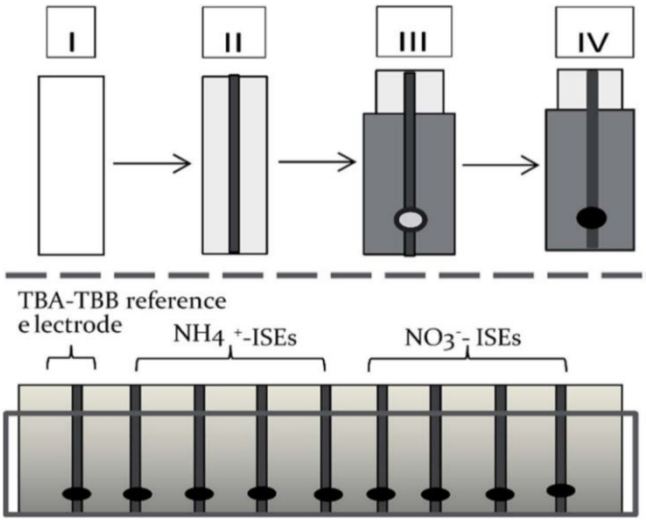

Fig. 2 Schematic representation of proposed acetate-based electrodes fabricated via mechanical abrasion. (Top) Step I: acetate sheet slightly roughened by sandpaper. Step II: line was drawn using a typical household pencil. Step III: insulating the platform using simple sellotape leaving only a small opening at the distal end of the electrode. Step IV: drop casting suitable cocktail. (Bottom) Finished single strip potentiometric device where one electrode was used for deposition of all-solid-contact reference electrode based on tetrabutylammonium tetrabutylborate (TBA-TBB), while the rest are used for deposition of the cocktails for required ISEs. Reproduced from ref. 78 with permission from the Royal Society of Chemistry, copyright 2017.

In addition to graphene materials, other carbons have also been investigated as ion-to-electron transducer of potentiometric nitrate sensors. Paczosa-Bator et al.[57, 74] developed the all-solid-state nitrate-selective electrodes using different types of nanosized carbon black as the transducer layer. Their results indicated that the high BET surface of carbon black particles improved the long-term potential stability of the sensors. The effect of average particle size between 25 and 60 nm on the potential reproducibility was also studied, which showed that larger carbon black particles led to better potential reproducibility. Furthermore, no significant water layer was detected between the ion-selective membrane and the solid-contact layer. The significance of this work was the development of high-performance nitrate sensor with a low-cost material, which is highly desirable for practical applications. Similarly, Fayose et al.[78] demonstrated a facile approach for preparing ultra-simple and inexpensive ISE platforms for simultaneously detection of nitrate and ammonium using commonly accessible household pencil as graphite source. Fig. 2 shows the preparation process of the all-solid-state pencil-drawn ISE electrodes and RE. The graphite via mechanical abrasion served as both ion-to-electron transducer and conductive substrate. The performances of the proposed platform for nitrate sensing are comparable with many other systems as shown in Table 3, although no data were provided on potential drift and the lifetime for nitrate detection.

Conductive polymers have also been employed as the ISE transducer layer for nitrate sensing. Schwarz et al.[79] reported a solid-contact ISE using in-situ electropolymerised polypyrrole (PPy) as the

transducer layer between the graphite paste substrate and PVC-based ISM. The low-cost ISE showed similar linear range and LOD to that constructed from the carbon-based materials for detection of nitrate in tap and well waters. Furthermore, it was proposed that a 6-12 months lifetime could be achieved in the pH range of 3-8 under laboratory conditions.

3.2 Nitrate in seawater

Voltammetric/amperometric sensors for nitrate detection in seawater have not been extensively studied, mainly because the LODs obtained were usually above 1 µM (Table 2), which is higher than the nitrate concentrations found in seawater matrix, particularly for the seawater at the ocean surface where the concentration of nitrate is at a nanomolar level.[91] Considering the near neutral condition and high chloride content of seawater, silver has been preferred as catalyst for design of voltammetric nitrate sensors. Legrand et al.[38] developed an electrode by electrodepositing silver nanoparticles on gold disc electrode to test nitrate in synthetic seawater. The sensor showed a linear range of 0.39-50 µM and limit of quantification of 0.39 µM. The peak current intensity remained at 95% of the initial value after regular detection of 25 µM nitrate for about 26 days. However, the information on the size of silver particles and formation of aggregates were not provided, which would be helpful for understanding the effect of silver nanoparticles on the sensing performances. Recently, Lebon et al.[39] reported an *in situ* metalorganic deposition method to modify the gold substrate with silver nanoparticles for catalytic detection of nitrate (Fig. 3A). This new deposition method was advantageous over conventional electrodeposition as extremely small silver nanoparticles with an average size of 4 nm was controllably modified on the gold grains of the electrode with good dispersity (Fig. 3B and C). Using SWV technique, the modified electrode exhibited a good linearity from 1 nM to 1000 µM and a LOD of 0.9 nM, which made it applicable for real seawater test. Compared with the silver particles prepared by electrodeposition method, the silver nanoparticles obtained by metalorganic deposition showed enhanced electrocatalytic activity towards nitrate reduction, which was evidenced by the remarkable decrease of the reduction peak potential from -1.1 V to -0.85 V, due to the well-dispersed small nanoparticles.[37, 38] It demonstrates that the morphology, size, and surface repartition of silver catalyst are key factors to design voltammetric and amperometric sensors for detection of nitrate in seawater matrix.

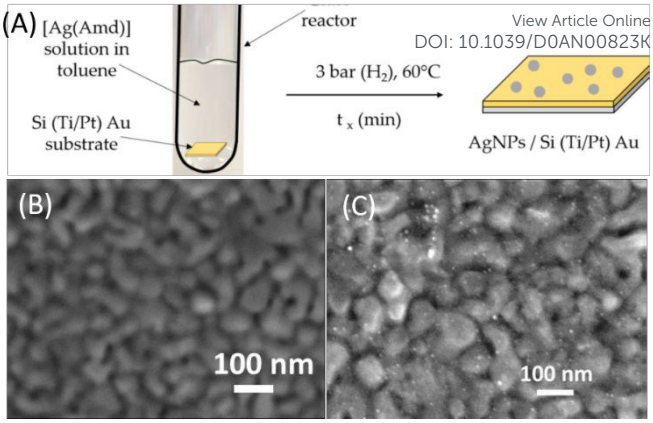

Fig. 3 (A) scheme of the *in situ* deposition of silver nanoparticles by the direct decomposition of silver precursor [Ag(Amd)] in solution in the presence of the Si(Ti/Pt)Au substrate; and filed emission gun scanning electron microscopy (FEG-SEM) image of the gold substrate without silver nanoparticles (B) and with silver nanoparticles (C) obtained with of [Ag(Amd)] = 0.04 mol/L, duration of [Ag(Amd)] decomposition = 1 min. Reproduced from ref. 39 with permission from MDPI, copyright 2018.

For the determination of nitrate in seawater using the potentiometric technique, the main barrier is the interferences from chloride. Bakker's group has conducted a series of studies to reduce the chloride interferences by pre-treating seawater with the in-line

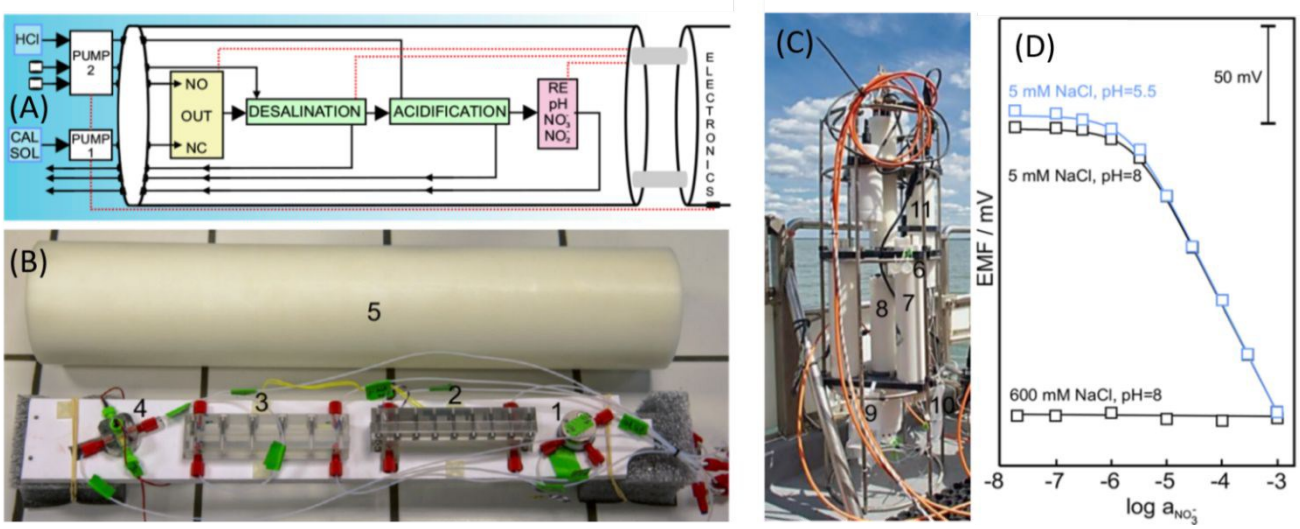

Fig. 4 (A) Scheme of the developed fluidics for in situ measurements (NO = normally open, NC = normally closed, CAL SOL = calibration solution, RE = reference electrode). (B) Image of the submersible probe based on the valve (1), the desalination module (2), the acidification module (3) and the potentiometric flow cell (4). The system is placed inside the water- and pressure-proof cylindrical housing (5) made of acetylic copolymer. (C) Probe incorporated into the titanium cage together with the pump and the CTD multiparemeter probe (6, filter for seawater; 7, pump; 8, unit containing the electrochemical sensors; 9, bag containing the calibration solution; 10, bag containing the HCl solution; 11, CTD). (D) Calibration graph obtained for nitrate using the developed flow potentiometric cell based on miniaturised all-solid-state electrodes. Reproduced from ref. 81 with permission from the American Chemical Society, copyright 2018.

electrochemical desalination unit and/or acidification unit.[80, 81, 92, 93] The recently developed submersible potentiometric nitrate and nitrite sensors[81] incorporated the tandem desalination module, acidification module and potentiometric flow cell into the fluidics (Fig. 4A and B). The proposed submersible device was capable of autonomous operation during on-site deployment, with routines for repetitive measurements, data storage and management, as well as computer visualisation of the data in real time. The desalination module can reduce the concentration of chloride from 600 mM to below 5 mM when the potential of 800 mV was applied for 300 s. As a result, the background noise caused by the high concentration of chloride was reduced significantly, which enabled the detection of nitrate at micromolar level in seawater (Fig. 4D). Although the potentiometric flow cell was miniaturised, the entire submersible device (Fig. 4C) was still large due to the combination of other auxiliary components such as the filter system, pump and bags for calibration and acidification solutions. In addition, the desalination unit needs to be improved for long-term measurements with more than 30 desalination cycles. Therefore, further miniaturisation of the device with a more robust and stable desalination design is highly desirable for future applications.

3.3 Nitrate in food

Hafezi et al.[71] developed an amperometric sensor based on disposable pencil graphite electrode modified with electrodeposited copper nanostructures to test nitrate in extraction solutions of sausage, hot-dog and cheese. The nitrate sensor showed a linear range of 1-35 µM and a LOD of 0.59 µM. The results obtained for the real sample tests were in good agreement with those obtained by spectrophotometric method. However, there are some limitations including that the analysis had to be carried out in solution with pH of 2, and the stability required further improvement. Bagheri et al.[72] fabricated a voltammetric sensor based on copper nanoparticles-multiwall carbon nanotubes-reduced graphene oxide nanosheets (Cu/MWCNT/RGO), which can determine nitrate and nitrite individually or simultaneously at a pH of 3. The copper nanoparticles with a typical size ranging from 25 to 52 nm produced by electrodeposition were well dispersed on MWCNT/RGO (Fig. 5A), exhibiting high catalytic activity and facile electron transfer kinetics. This sensor achieved a low LOD of 20 nM with a linear range of 0.1-75 µM for nitrate detection (Fig. 5B and C). The analytical results were in good agreement with those obtained by classic Griess method when applied to test nitrate and nitrite in water extractions of sausage, salami and cheese. In addition, under neutral condition, Ghanbari[40] proposed a nitrate sensor based on silver nanoparticles dispersed in polypyrrole matrix on glassy carbon electrode for analysis of nitrate in sausage and cheese extraction solutions. The sensor retained 90% of the initial activity after one month, which can be attributed to the increase of effective surface area and the good stability of silver nanoparticles in the polypyrrole matrix.

An impressive study for detection of nitrate in food matrix was conducted by Andac et al,[82] who developed a flow injection potentiometric method for nitrate analysis in leafy vegetables. The miniaturised solid contact electrode showed a linear range of 100 µM to 0.1 M and a LOD of 66 µM. Although these performances were not outstanding compared with those obtained from other sensors in Table 3, the combination of flow injection enabled the system to test

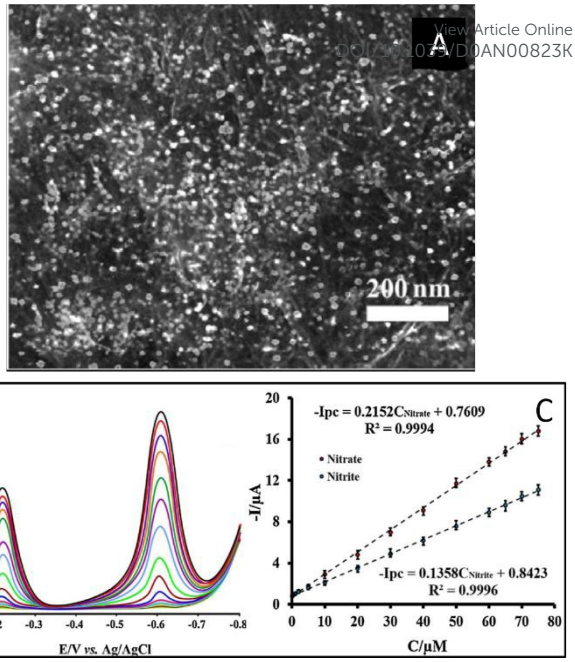

Fig. 5 (A) SEM image of Cu/MWCNT/RGO/GCE; (B) SWVs of Cu/MWCNT/RGO/GCE at various concentrations of nitrite and nitrate simultaneously (0.1, 0.2, 0.5, 1, 2, 5, 10, 20, 30, 40, 50, 60, 65, 70, and 75 µM) in Na2SO4/H2SO4 solution, pH = 3.0; (C) calibration curve of nitrate and nitrite based on peak currents from (B). Reproduced from ref. 72 with permission from Elsevier, copyright 2017.

90 samples per hour but consumed only 20 µL sample per injection. Wardak et al.[83, 84] developed a type of solid contact ISE by incorporating the ionic liquid of trihexyltetradecylphosphonium chloride (THTDPCl) into the ISM. THTDPCl played three roles as (i) ionophore for nitrate transfer across the ISM, (ii) lipophilic ionic component for the reduction of the membrane resistance and (iii) transducer media for the stabilisation of the internal Ag/AgCl electrode potential which in turn resulted in high potential stability and reversibility. This potentiometric sensor showed reliable and stable performances with a lifetime of 4 months under pH range of 3-10 for testing nitrate from 10 µM to 0.1 M in iceberg lettuce, butterhead lettuce and fresh spinach.

3.4 Nitrate in soil

One of the biggest challenges of detecting nitrate in soil matrix is to realise real-time and in-field measurement. In this regard, potentiometric sensors are advantageous over the voltammetric/amperometric sensors due to the less requirements on sample pre-treatments.[94] Zhang et al.[85] presented two solid-state ISEs consisting of graphene (TG-NS) or electropolymerised pyrrole (PPy-NS) as the transducer layer between the glassy carbon and ISM to monitor nitrate in the soil extract and slurry. The results demonstrated that the potential response observed from the TG-NS-based ISE was faster and more stable than that of the PPy-NS-based one. However, unstable potential drifting occurred to both ISEs when tested in the soil slurry, which could limit their on-site applications.

Garland et al.[86] build a miniaturised flexible all-solid-state sensing platform for testing nitrate and ammonium in soil slurry and soil column. As shown in Fig .6, the ISE was fabricated by applying classical PVC-based ISM onto laser-induced graphene (LIG) formed on polyimide substrate, and the RE was made of Ag/AgCl paint. The

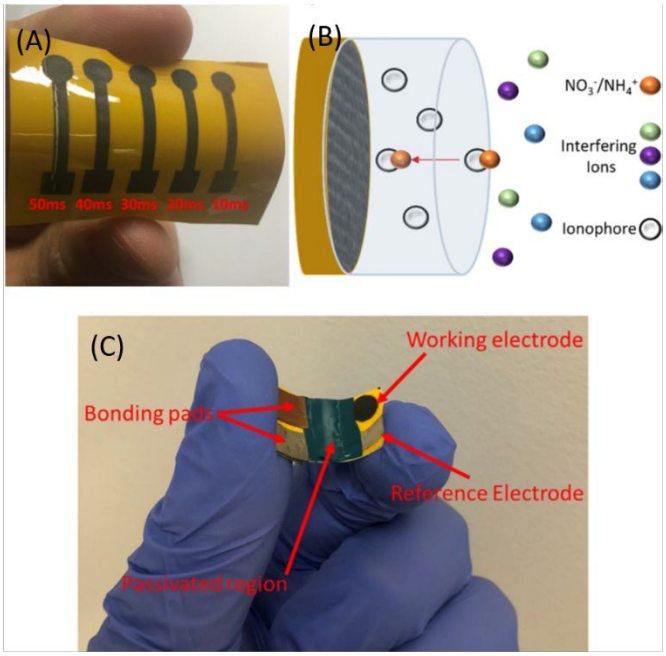

Fig. 6 (A) Photograph of five LIG SC ISEs on a single polyimide swatch. (B) Illustration of SC-ISE ion sensing. (C) Representative electrode used in soil column studies. Passivated regions are shown as well as bonding pads, working electrode, and reference electrode. Reproduced from ref. 86 with permission from the American Chemical Society, copyright 2018.

LIG was formed by irradiating a thin sheet of polyimide with a laser, which photothermally converted polyimide at the surface to sp^2-hybridised carbon.[95] The one-step method for graphene fabrication is much less expensive than the traditional chemical vapor deposition. The LIG-based ISEs showed a linear range from 10 µM to 0.1 M with a LOD of 20.6±14.8 µM for nitrate determination. Furthermore, no degradation in sensor response associated with the existence of a water layer between the ISM and the LIG was observed. The all-solid-state sensing platform has been successfully used to determine nitrate in soil slurry and soil column with satisfactory recovery of over 95%. These performances were comparable to those of the commercial nitrate electrodes, though the precision could be improved further. The most attractive feature of the LIG-based ISEs is that they are amenable to scalable roll-to-roll manufacturing, which is promising for the development of cost-effective and disposable sensors for on-site monitoring of nitrate.

Recently, Ali et al. developed a miniaturised all-solid-state nitrate sensor, which was fabricated on a printed circuit board (PCB) using patterned working electrode (i.e. ISE) and RE.[87] Fig. 7 shows the brief fabrication process, the finished sensing device and the working principle. The ISE was built on top of a copper pad of a PCB covered by a thin, patterned gold (Au) layer, a solid-contact layer of poly(3-octyl-thiophene) and molybdenum disulfide (POT–MoS_2) nanocomposite, and a nitrate-specific ISM. The nitrate sensing results showed that the POT–MoS_2-based ISE had lower potential drift and higher sensitivity compared with the POT or MoS_2 electrode, which may be ascribed to the high hydrophobicity and good redox properties of the POT–MoS_2 nanocomposites. The RE consisted of a screen-printed Ag/AgCl electrode prepared by placing a stencil mask on top of the PCB. Subsequently, a Nafion layer, which could prevent chloride leaching, was coated on the Ag/AgCl electrode to minimise

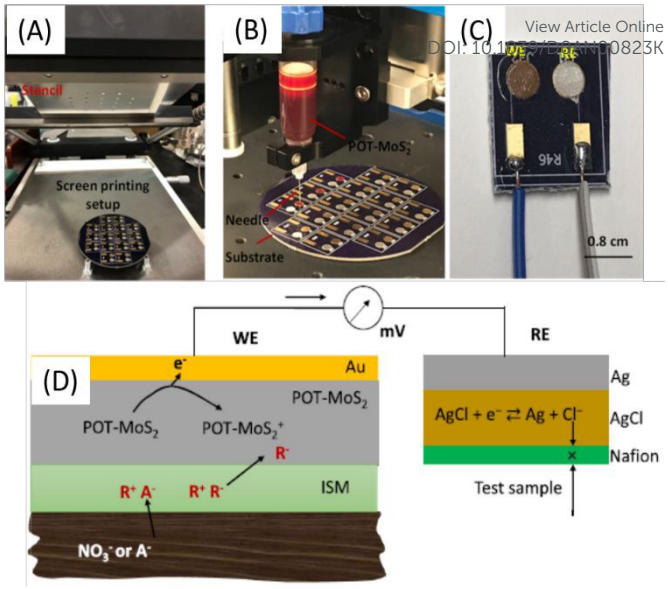

Fig. 7 (A) - (C) Stepwise representation of the fabrication of all-solid-state soil nitrate sensor: (A) Photograph taken during printing Ag/AgCl paste on circular-shaped Ag electrodes using a stencil printer. (B) Photograph taken during materials dispensing (POT–MoS_2 in THF solvent) on circular-shaped Au electrodes using a programmable high-precision automated fluid-dispensing robot. (C) Photograph of the device. (D) Oxidation process for the WE (ISM/POT–MoS_2/Au) in the presence of soil solution NO_3^- ions. R^+ and R^- represent the anion and cation exchangers at the organic membrane, and M^+ and A^- are the hydrophilic ions in soil water. POT–MoS_2 and POT–MoS_2^+ indicate neutral and oxidised POT–MoS_2 units, respectively. Oxidation/reduction is shown for the Ag/AgCl RE. Reproduced from ref. 87 with permission from the American Chemical Society, copyright 2019.

the drift of reference potential that usually occurred to the bare Ag/AgCl RE.[86] Although the LOD of the proposed nitrate sensor was relatively high, it exhibited a wide linear range (1-1500 ppm) and good accuracy. The sensor system was used in a soil column for a duration of 27 days with relatively stable potential response.

3.5 Nitrate in particulate matter

Particulate matter (PM) is currently receiving extensive research interest due to its negative impacts on the climate change, the biogeochemical cycles, the chemistry of the atmosphere, as well as human health.[96] Nitrate is a major component of PM2.5, which is a common air pollutant with the aerodynamic diameter of less than 2.5 µm.[97] Yu et al.[24] used a copper-modified carbon fibre microdisc electrode to detect nitrate in the extracted solution of PM2.5 with a pH of 2. The results were in good agreement with those obtained by ion chromatography. This voltammetric sensor showed a LOD of 1.1 µM with a linear range of 3-2000 µM, while Cu^{2+} and Cl^- must be added into the sample solution to obtain satisfactory performances. To date, little effort has been devoted to in-situ measurement of nitrate in PM. Clearly, much more can be done in this area.

4. Conclusions and Perspective

Electrochemical sensors for nitrate analysis have been explored for over 40 years. Although the electrochemical techniques were well established, new devices fabricated from novel materials with improved analytical performances for various applications have emerged in recent years. This review has focused on the recent advances in electrochemical nitrate

sensors developed for applications in food and environmental matrices. Special emphasis is given to the matrix as it dictates the selection of fit-for-purpose electrochemical techniques and electrode materials, particularly for in-field deployment of the sensing devices. Taking nitrate detection in seawater as an example, the voltammetric sensors with well-dispersed silver nanoparticles as catalysts are preferred to the potentiometric sensors due to the higher sensitivity, much lower LOD and anti-interference capability from chloride. In contrast, potentiometric sensors with miniaturised flexible all-solid-state ISEs, which require little or no sample pre-treatment, would be more suitable for in-field measurement of nitrate in soil matrix.

Owing to the high sensitivity of electrochemical techniques, the LODs of the sensors described in Table 2 and 3 are much lower than the nitrate guideline levels proposed by different countries and regions (Table 1). This means that electrochemical sensors have sufficient capability to evaluate the risk of nitrate exposure from food and drinking water, coupled with the ease of operation and miniaturisation, making them promising candidates as nitrate test kit for environmental health and safety applications. The key challenges in future development of electrochemical nitrate sensors include the achievement of accuracy, long-term stability and the enhancement of anti-interference ability. Electrode surface fouling is also a common problem in electrochemical measurements of nitrate in complex media, such as milk, soil and wastewater. The fouling process could cause passivation of the sensing interface and/or signal drift, resulting in a loss of sensitivity, stability and reproducibility. Thus, electrodes must be cleaned and calibrated frequently, which is time-consuming and labour-intensive. In order to address these challenges, development of low-cost and miniaturised disposable nitrate sensors with good accuracy will undoubtedly be one of the future directions to be pursued. While most current attentions in electroanalytical applications are on design of integrated sensing system to realise *in situ* and continuous detection of environmental pollutants, more efforts should be directed at exploring smart electrochemical devices that can remotely measure nitrate in real-time. To this end, integration of Internet of Things (IoT) with advanced functional materials offers the best possibilities. This will certainly also open new avenues for future applications of electrochemical nitrate sensors.

Conflicts of interest

There are no conflicts to declare.

Acknowledgements

The authors gratefully acknowledge the financial support from James Cook University and the Queensland Government (WRAP052-2019RD1).

References

1. N. G. Hord, Y. Tang and N. S. Bryan, *The American Journal of Clinical Nutrition*, 2009, **90**, 1-10.
2. M. H. Ward, *Rev Environ Health*, 2009, **24**, 357-363.
3. M. Gutiérrez, R. N. Biagioni, M. T. Alarcón-Herrera and B. A. Rivas-Lucero, *Science of The Total Environment*, 2018, **624**, 1513-1522.
4. K. Wick, C. Heumesser and E. Schmid, *J Environ Manage*, 2012, **111**, 178-186.
5. *Agency for Toxic Substances and Disease Registry*, https://www.atsdr.cdc.gov/csem/csem.asp?csem=28&po=8 (accessed Mar 2020).
6. *Council Directive 98/83/EC of 3 November 1998 on the quality of water intended for human consumption*, https://eur-lex.europa.eu/legal-content/EN/TXT/?uri=CELEX:31998L0083 (accessed Mar 2020).
7. E. Panel o. F. Additives, N. S. a. t. Food, A. Mortensen, F. Aguilar, R. Crebelli, A. Di Domenico, B. Dusemund, M. J. Frutos, P. Galtier, D. Gott, U. Gundert-Remy, C. Lambré, J.-C. Leblanc, O. Lindtner, P. Moldeus, P. Mosesso, A. Oskarsson, D. Parent-Massin, I. Stankovic, I. Waalkens-Berendsen, R. A. Woutersen, M. Wright, P. van den Brandt, C. Fortes, L. Merino, F. Toldrà, D. Arcella, A. Christodoulidou, F. Barrucci, A. Garcia, F. Pizzo, D. Battacchi and M. Younes, *EFSA Journal*, 2017, **15**, e04787.
8. *Australian Drinking Water Guidelines 6, Version 3.4, updated October 2017*, https://www.nhmrc.gov.au/sites/default/files/documents/reports/aust-drinking-water-guidelines.pdf (accessed Mar 2020).
9. *Australia New Zealand Food Standards Code – Schedule 15*, https://www.legislation.gov.au/Details/F2017C00331 (accessed Mar 2020).
10. *WHO Guidelines for Drinking-water Quality*, https://www.who.int/water_sanitation_health/water-quality/guidelines/chemicals/nitratesnitrite/en/ (accessed Mar 2020).
11. P. Jakszyn and C.-A. Gonzalez, *World J Gastroenterol*, 2006, **12**, 4296-4303.
12. C. Oertel, J. Matschullat, K. Zurba, F. Zimmermann and S. Erasmi, *Geochemistry*, 2016, **76**, 327-352.
13. M. Sohail and S. B. Adeloju, *Talanta*, 2016, **153**, 83-98.
14. Q.-H. Wang, L.-J. Yu, Y. Liu, L. Lin, R.-g. Lu, J.-p. Zhu, L. He and Z.-L. Lu, *Talanta*, 2017, **165**, 709-720.
15. M. E. E. Alahi and S. C. Mukhopadhyay, *Sensors and Actuators A: Physical*, 2018, **280**, 210-221.
16. X. Chen, G. Zhou, S. Mao and J. Chen, *Environmental Science: Nano*, 2018, **5**, 837-862.
17. O. Korostynska, A. Mason and A. Al-Shamma'a, *International Journal on Smart Sensing & Intelligent Systems*, 2012, **5**, 149-176.
18. A. Azmi, A. A. Azman, S. Ibrahim and M. A. M. Yunus, *International Journal on Smart Sensing & Intelligent Systems*, 2017, **10**, 224-261.
19. A. C. Michael and L. Borland, *Electrochemical methods for neuroscience*, CRC press, 2006.
20. V. Rosca, M. Duca, M. T. de Groot and M. T. M. Koper, *Chemical Reviews*, 2009, **109**, 2209-2244.
21. J. Martínez, A. Ortiz and I. Ortiz, *Applied Catalysis B: Environmental*, 2017, **207**, 42-59.
22. S. Garcia-Segura, M. Lanzarini-Lopes, K. Hristovski and P.

Westerhoff, *Applied Catalysis B: Environmental*, 2018, **236**, 546-568.
23. G. E. Dima, A. C. A. de Vooys and M. T. M. Koper, *Journal of Electroanalytical Chemistry*, 2003, **554-555**, 15-23.
24. L. Yu, Q. Zhang, Q. Xu, D. Jin, G. Jin, K. Li and X. Hu, *Talanta*, 2015, **143**, 245-253.
25. J. Liang, Y. Zheng and Z. Liu, *Sensors and Actuators B: Chemical*, 2016, **232**, 336-344.
26. N. G. Carpenter and D. Pletcher, *Analytica Chimica Acta*, 1995, **317**, 287-293.
27. J. Davis, M. J. Moorcroft, S. J. Wilkins, R. G. Compton and M. F. Cardosi, *Analyst*, 2000, **125**, 737-742.
28. I. S. da Silva, W. R. de Araujo, T. R. L. C. Paixão and L. Angnes, *Sensors and Actuators B: Chemical*, 2013, **188**, 94-98.
29. A. M. Stortini, L. M. Moretto, A. Mardegan, M. Ongaro and P. Ugo, *Sensors and Actuators B: Chemical*, 2015, **207**, 186-192.
30. Y. Li, H. Han, D. Pan and P. Zhang, *Journal of The Electrochemical Society*, 2019, **166**, B1038-B1043.
31. F. Can, S. Korkut Ozoner, P. Ergenekon and E. Erhan, *Materials Science and Engineering: C*, 2012, **32**, 18-23.
32. R. Ahmad, K. S. Bhat, M.-S. Ahn and Y.-B. Hahn, *New Journal of Chemistry*, 2017, **41**, 10992-10997.
33. F. Manea, A. Remes, C. Radovan, R. Pode, S. Picken and J. Schoonman, *Talanta*, 2010, **83**, 66-71.
34. D.-L. Zhou, Q.-L. Zhang, Z.-Y. Lv, W.-Y. Chen, X.-F. Liu, Y.-H. Lu, A.-J. Wang and J.-J. Feng, *Microchimica Acta*, 2013, **180**, 1495-1500.
35. J. Hu, J. Sun, C. Bian, J. Tong and X. Shanhong, *Electroanalysis*, 2013, **25**, 546-556.
36. H. R. Lotfi Zadeh Zhad and R. Y. Lai, *Analytica Chimica Acta*, 2015, **892**, 153-159.
37. K. Fajerwerg, V. Ynam, B. Chaudret, V. Garçon, D. Thouron and M. Comtat, *Electrochemistry Communications*, 2010, **12**, 1439-1441.
38. D. Chen Legrand, C. Barus and V. Garçon, *Electroanalysis*, 2017, **29**, 2882-2887.
39. E. Lebon, P. Fau, M. Comtat, M. L. Kahn, A. Sournia-Saquet, P. Temple-Boyer, B. Dubreuil, P. Behra and K. Fajerwerg, *Chemosensors*, 2018, **6**, 50.
40. K. Ghanbari, *Anal Bioanal Electrochem*, 2013, **5**, 46-58.
41. M.-C. Tsai, D.-X. Zhuang and P.-Y. Chen, *Electrochimica Acta*, 2010, **55**, 1019-1027.
42. M. Bonyani, A. Mirzaei, S. G. Leonardi and G. Neri, *Measurement*, 2016, **84**, 83-90.
43. L. Guadagnini and D. Tonelli, *Sensors and Actuators B: Chemical*, 2013, **188**, 806-814.
44. M. Atmeh and B. E. Alcock-Earley, *Journal of Applied Electrochemistry*, 2011, **41**, 1341.
45. E. Andreoli, V. Annibaldi, D. A. Rooney, K.-S. Liao, N. J. Alley, S. A. Curran and C. B. Breslin, *Electroanalysis*, 2011, **23**, 2164-2173.
46. A. Gutés, C. Carraro and R. Maboudian, *Electrochimica Acta*, 2013, **103**, 38-43.
47. N. Comisso, S. Cattarin, P. Guerriero, L. Mattarozzi, M. Musiani, L. Vázquez-Gómez and E. Verlato, *Journal of Solid State Electrochemistry*, 2016, **20**, 1139-1148.
48. N. Plumeré, J. Henig and W. H. Campbell, *Analytical Chemistry*, 2012, **84**, 2141-2146.
49. N. Plumeré, *Analytical and Bioanalytical Chemistry*, 2013, **405**, 3731-3738.
50. K. Zhang, H. Zhou, P. Hu and Q. Lu, *RSC Advances*, 2019, **9**, 37207-37213.
51. M. Paidar, I. Roušar and K. Bouzek, *Journal of Applied Electrochemistry*, 1999, **29**, 611-617.
52. C. Milhano and D. Pletcher, in *Modern Aspects of Electrochemistry, No. 45*, ed. R. E. White, Springer New York, New York, NY, 2009, DOI: 10.1007/978-1-4419-0655-7_1, pp. 1-61.
53. E. Zdrachek and E. Bakker, *Analytical Chemistry*, 2019, **91**, 2-26.
54. M. Cuartero and G. A. Crespo, *Current Opinion in Electrochemistry*, 2018, **10**, 98-106.
55. J. Hu, A. Stein and P. Bühlmann, *TrAC Trends in Analytical Chemistry*, 2016, **76**, 102-114.
56. D. Yuan, A. H. C. Anthis, M. Ghahraman Afshar, N. Pankratova, M. Cuartero, G. A. Crespo and E. Bakker, *Analytical Chemistry*, 2015, **87**, 8640-8645.
57. B. Paczosa-Bator, *Microchimica Acta*, 2014, **181**, 1093-1099.
58. M. Sophocleous and J. K. Atkinson, *Sensors and Actuators A: Physical*, 2017, **267**, 106-120.
59. Y. Liu, Y. Liu, Z. Meng, Y. Qin, D. Jiang, K. Xi and P. Wang, *Talanta*, 2020, **208**, 120374.
60. A. S. Watts, V. G. Gavalas, A. Cammers, P. S. Andrada, M. Alajarín and L. G. Bachas, *Sensors and Actuators B: Chemical*, 2007, **121**, 200-207.
61. D. Wegmann, H. Weiss, D. Ammann, W. E. Morf, E. Pretsch, K. Sugahara and W. Simon, *Microchimica Acta*, 1984, **84**, 1-16.
62. B. Néel, M. Ghahraman Asfhar, G. A. Crespo, M. Pawlak, D. Dorokhin and E. Bakker, *Electroanalysis*, 2014, **26**, 473-480.
63. B. Sun and P. G. Fitch, *Electroanalysis*, 1997, **9**, 494-497.
64. T. Le Goff, J. Braven, L. Ebdon and D. Scholefield, *Analytical Chemistry*, 2002, **74**, 2596-2602.
65. A. C. A. de Vooys, R. A. van Santen and J. A. R. van Veen, *Journal of Molecular Catalysis A: Chemical*, 2000, **154**, 203-215.
66. O. Ghodbane, M. Sarrazin, L. Roué and D. Bélanger, *Journal of The Electrochemical Society*, 2008, **155**, F117-F123.
67. Y. Li, J. Sun, C. Bian, J. Tong and S. Xia, *Procedia Engineering*, 2010, **5**, 339-342.
68. I. S. da Silva, W. R. de Araujo, T. R. Paixão and L. Angnes, *Sensors and Actuators B: Chemical*, 2013, **188**, 94-98.
69. T. Öznülüer, B. Özdurak and H. Öztürk Doğan, *Journal of Electroanalytical Chemistry*, 2013, **699**, 1-5.
70. J. C. Gamboa, R. C. Pena, T. R. Paixão and M. Bertotti, *Talanta*, 2009, **80**, 581-585.
71. B. Hafezi and M. R. Majidi, *Analytical Methods*, 2013, **5**, 3552-3556.
72. H. Bagheri, A. Hajian, M. Rezaei and A. Shirzadmehr, *Journal of Hazardous Materials*, 2017, **324**, 762-772.
73. W. Tang, J. Ping, K. Fan, Y. Wang, X. Luo, Y. Ying, J. Wu and Q. Zhou, *Electrochimica Acta*, 2012, **81**, 186-190.
74. B. Paczosa-Bator, L. Cabaj, R. Piech and K. Skupień, *Analytical chemistry*, 2013, **85**, 10255-10261.
75. M. Pięk, R. Piech and B. Paczosa-Bator, *Journal of The Electrochemical Society*, 2015, **162**, B257-B263.
76. M. Pięk, R. Piech and B. Paczosa-Bator, *Electrochimica Acta*, 2016, **210**, 407-414.
77. M. Pięk, R. Piech and B. Paczosa-Bator, *Journal of The Electrochemical Society*, 2018, **165**, B60-B65.
78. T. Fayose, L. Mendecki, S. Ullah and A. Radu, *Analytical Methods*, 2017, **9**, 1213-1220.

View Article Online
DOI: 10.1039/D0AN00823K

79. J. Schwarz, K. Trommer and M. Mertig, *American Journal of Analytical Chemistry*, 2018, **9**, 591-601.
80. M. Cuartero, G. A. Crespo and E. Bakker, *Analytical Chemistry*, 2015, **87**, 8084-8089.
81. M. Cuartero, G. Crespo, T. Cherubini, N. Pankratova, F. Confalonieri, F. Massa, M.-L. Tercier-Waeber, M. Abdou, J. Schäfer and E. Bakker, *Analytical Chemistry*, 2018, **90**, 4702-4710.
82. M. Andac, H. Eren and F. Coldur, *Journal of Food and Drug Analysis*, 2011, **19**, 457-462.
83. C. Wardak, *Electroanalysis*, 2014, **26**, 864-872.
84. C. Wardak and M. Grabarczyk, *Journal of Environmental Science and Health, Part B*, 2016, **51**, 519-524.
85. L. Zhang, M. Zhang, H. Ren, P. Pu, P. Kong and H. Zhao, *Computers and Electronics in Agriculture*, 2015, **112**, 83-91.
86. N. T. Garland, E. S. McLamore, N. D. Cavallaro, D. Mendivelso-Perez, E. A. Smith, D. Jing and J. C. Claussen, *ACS applied materials & interfaces*, 2018, **10**, 39124-39133.
87. M. A. Ali, X. Wang, Y. Chen, Y. Jiao, N. K. Mahal, S. Moru, M. J. Castellano, J. C. Schnable, P. S. Schnable and L. Dong, *ACS Applied Materials & Interfaces*, 2019, **11**, 29195-29206.
88. D. Pan, W. Lu, H. Zhang, L. Zhang and J. Zhuang, *International Journal of Environmental Analytical Chemistry*, 2013, **93**, 935-945.
89. L. Mattarozzi, S. Cattarin, N. Comisso, A. Gambirasi, P. Guerriero, M. Musiani, L. Vázquez-Gómez and E. Verlato, *Electrochimica Acta*, 2014, **140**, 337-344.
90. S. S. Hassan, *Talanta*, 1976, **23**, 738-740.
91. M. D. Patey, M. J. A. Rijkenberg, P. J. Statham, M. C. Stinchcombe, E. P. Achterberg and M. Mowlem, *TrAC Trends in Analytical Chemistry*, 2008, **27**, 169-182.
92. N. Pankratova, M. Ghahraman Afshar, D. Yuan, G. A. Crespo and E. Bakker, *ACS Sensors*, 2016, **1**, 48-54.
93. N. Pankratova, M. Cuartero, T. Cherubini, G. A. Crespo and E. Bakker, *Analytical Chemistry*, 2017, **89**, 571-575.
94. J. V. Sinfield, D. Fagerman and O. Colic, *Computers and Electronics in Agriculture*, 2010, **70**, 1-18.
95. J. Lin, Z. Peng, Y. Liu, F. Ruiz-Zepeda, R. Ye, E. L. Samuel, M. J. Yacaman, B. I. Yakobson and J. M. Tour, *Nature communications*, 2014, **5**, 5714.
96. S. Fuzzi, U. Baltensperger, K. Carslaw, S. Decesari, H. Denier van der Gon, M. C. Facchini, D. Fowler, I. Koren, B. Langford and U. Lohmann, *Atmospheric chemistry and physics*, 2015, **15**, 8217-8299.
97. R. M. Harrison, A. M. Jones and R. G. Lawrence, *Atmospheric Environment*, 2004, **38**, 4531-4538.

View Article Online
DOI: 10.1039/D0AN00823K

Table of Content

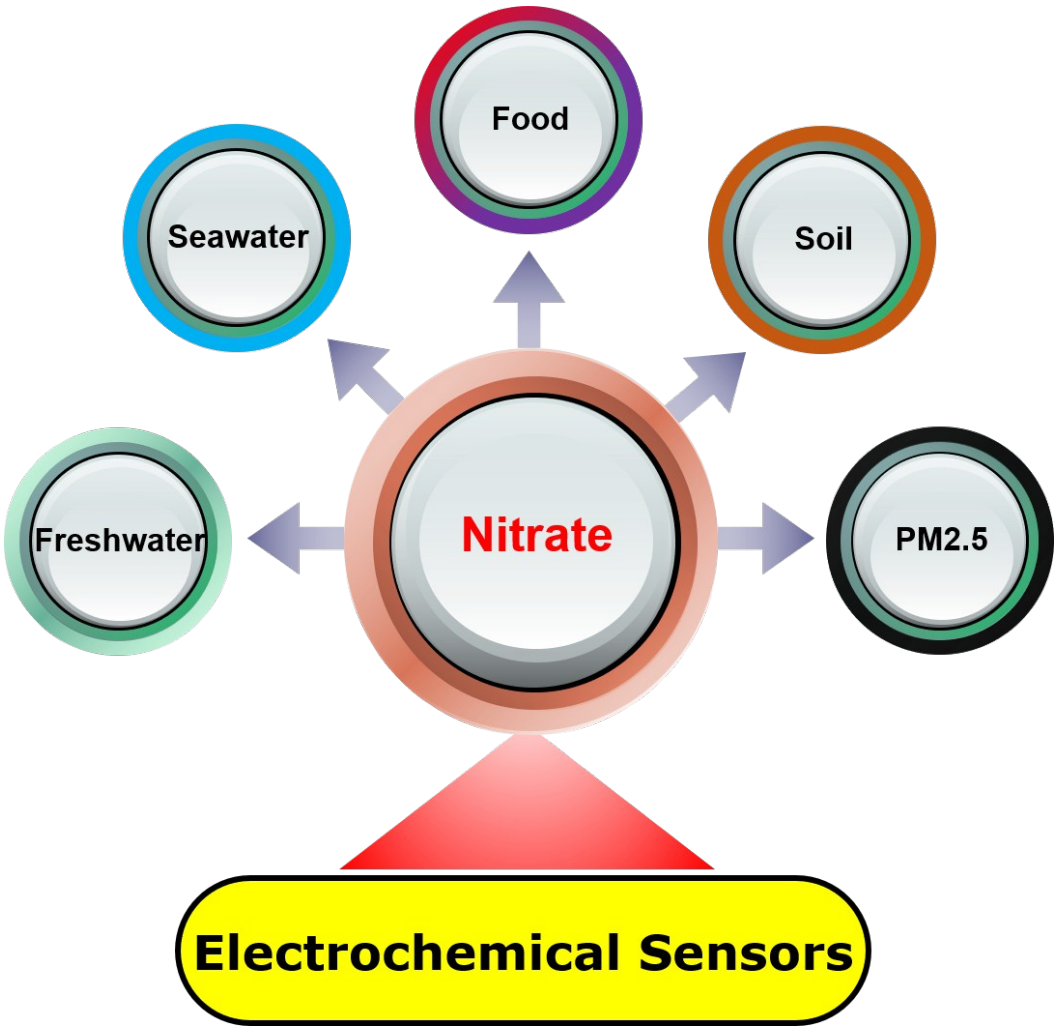

Electrochemical determination of nitrate: an overview from the perspective of sample matrix.